Design and Development of Multibeam Antenna Technologies for 5G Wireless Communications

Freddy Patricio Ajila Zaquinaula [a*]& Rolando Marcel Torres Castillo[a]
[a]Escuela Superior Politécnica de Chimborazo, Sede Orellana, El Coca, 220001, Ecuador

Abstract:
Multibeam antenna (MBA) systems operating in the millimeter-wave frequency bands have drawn significant attention from researchers and are being effectively studied due to the demanding system needs for the fifth-generation (5G) wireless communication systems and the drastic spectrum scarcity at the existing cellular frequency range. To enable a greater transmission speed, an enhanced signal-to-interference-plus-noise ratio, an enhanced spectral and energy performance, and flexible beam shaping, they serve as the primary antenna technology. They offer tremendous potential for serving as the crucial infrastructure for facilitating beamforming and massive multiple-input multiple-output (MIMO) which uplift the 5G. To achieve this, a novel beamforming design and optimization approach based on the Convex Time Modulated Particle Swarm Optimization (CTM-PSO) algorithm is suggested for 5G communication networks, offering multiple concurrent transceivers to support efficient beamformed interactions whereas a second beam concurrently detects the atmosphere around the base-station. The suggested beamforming method combines the optimization of the transmitter and receiver beamforming weights to increase sensor performance, reduce potential intervention resulting from the communication beams, and ensure the communications link's target beamforming gains. Comprehensive numerical assessments are used to evaluate the effectiveness of the recommended method, showing that it may provide significant improvements over more conventional beamforming methods.
Keywords: Multibeam antenna, fifth-generation (5G), beamforming, Convex Time Modulated Particle Swarm Optimization (CTM-PSO) algorithm
DOI: 10.24297/j.cims.2023.19

1. Introduction

Fifth Generation (5G) Communication refers to the most current wave of cellular telecommunications in the field of wireless transmission. More notably, throughout the last thirty years, there has been a perceptible increase in the rate of fast development in the area of wireless transmission about the migration from 1G to 4G. The need for huge bandwidth and extremely minimal delay served as the primary motivating factor for this study. 5G promises to offer a fast information throughput, enhanced service quality, reduced latency, great coverage, high dependability, and financially accessible capabilities (Dangi et al. (2021)). Innovative

developing technologies must be blended to provide a variety of prospective capabilities for enhanced communications systems. It is generally agreed that this objective can only be attained by the simultaneous implementation of 5G wireless and optical technologies. Because of its potential to enhance and modernize day-to-day living, the scientific community is paying a lot of focus to the emerging concept of many inventions, which are made possible by 5G mobile technologies and the urban growth of cellular networks (Miladić et al. (2021)). 5G provides services that may be broken down into the following categories: 1. Extreme mobile bandwidth (eMB). High-speed internet access, UltraHD broadcasting movies, virtual environment, and augmented environment media, among other things, are all provided by this non-standalone technology. The 3GPP produces a standard for massive machine-type connectivity in its 13th edition. It offers low-cost, wide-bandwidth machine-type connectivity across great distances with minimal energy usage. It offers mobile operators for IoT systems a fast information rate solution, low energy, higher bandwidth, and fewer complicated devices. 3. Unlike standard mobile network design, ultra-reliable low latency connectivity delivers reduced delay, ultra-high dependability, and greater service quality. It is intended for real-time, on-demand operations such as those in intelligent transportation systems, industry 4.0, digital infrastructures, telemedicine, etc (Njoku et al. (2022)). The next generation of commercial and non-terrestrial mobile connectivity systems will rely heavily on multi-beam antennae as essential elements. The many beams that are created by these transmitters will make it possible for distinct domestic, aerial, and space-borne network elements to be dynamically interconnected with one another. It is anticipated that high millimeter wave (mmWave) and terahertz (THz) bands would increasingly predominate in the creation of powerful amplification multi-beam antennas as the operational bandwidth for 5G and beyond 5G (B5G) systems grows to these bands (Guo et al. (2021)). Multibeam antenna arrays, which provide unparalleled connection and excellent spectrum effectiveness, are at the basis of 5G and beyond 5G (B5G) technologies. The most adaptable method for producing independently directional multiple beams is electronic beamforming, which includes Multiple-Input-Multiple-Output (MIMO) digital signals. Unquestionably, completely digital beamforming using enormous antenna arrays is a potent technology that can handle some of the most difficult requirements for prospective wireless transmission networks, especially in situations with a lot of dispersion. This method, meanwhile, often results in significant energy usage and equipment costs, which exclude its usage in situations like large bandwidth minimal cost connectivity as well as smaller aerial and space-borne vehicles with constrained power supplies. Nevertheless, as line of sight (LoS) wave transmission becomes more prevalent at greater mm-wave and terahertz (THz) frequencies, they are more adapted for

these frequencies. Digital multiple beam directional antennas relying on beamforming networks are a cost- and energy-effective technology ideally suited for the microwaves sector (Guo et al. (2021)). In most industrial 5G transmission systems, numerous fixed or hopped beams are used, and co-channel disturbance control is not always present. The newest artwork, however, shows that phasing arrays are also being examined for commercial spacecraft uses. Recent innovations of antenna array systems have appeared in wireless networking with the introduction of 5G/6G and the allotment of frequency in the mm-wave spectrum for increased throughput. Dynamic integrating designs, which can only produce one beam at a time and were developed by several networks, are some examples of cutting-edge base station antennas. Realistic multibeam antennas are still a long way off in the professional high-volume mm-wave 5G industry because of a variety of practical considerations including price, design specifications, dissipation, and processing load. Although there are numerous instances of mm-wave receivers that use simultaneous beams and chip scale fusion beamforming and have a limited number of components (Guo et al. (2022)). Consequently, increased adaptability, frequency recycling (by spatial modulation), and energy conservation at low terrestrial and space sectors will be necessary for both mobile and satellite telecommunications in the coming years. The antenna problems are to prevent side lobe disturbance buildup at each end, which occurs in existing systems using multiple beam forming grids, and to minimize performance and energy efficient damages suffered by array amplitude fades and beam pass. Moreover, forthcoming satellite technology at the space and surface sections will need effective and adaptable dynamic multiple beam formation with co-channel disturbance reduction. Similar requirements for several beamforming and minimal disturbance apply to 5G mobile communications ground stations and user devices (Aslan et al. (2021)).

Therefore, we proposed a novel beamforming optimization and configuration model based on the Convex Time Modulated Particle Swarm Optimization (CTM-PSO) algorithm for 5G communication networks to overcome the drawback in 5G communication and facilitate an increased transmission rate, reduced latency, an augmented spectral and negligible energy consumption, and adjustable beam shaping.

The remainder of the paper is divided into the following parts. Section II presents the relevant literature as well as the problem statement. Section III explains the suggested work. Performance analysis is included in Section IV. Section V contains the conclusion of the suggested paper.

2. Literature Review

Ruggerini et al. (2019) discussed the development, production, and evaluation of a Ka-band broadcasting actively discontinuous lens antenna prototype. Such antennae have great aspects involved, a large bandwidth spectrum, and the ability to provide multi-beam covering with only one primary reflector. Although beamforming is mostly accomplished in available space, the antenna's complexities and price increase only a little as the number of beams and radiative components increases (Vallappil et al. (2020)). To fulfill the increasing network requirement, the 5th generation wireless networks' technical advancements will be required. Connection speeds of close to 10Gbps, 1-ms delay, and lower energy consumption are all features of 5G communication systems. It is well recognized that 5G wireless networks will make use of frequencies outside of the 3 GHz microwaves and millimeter-wave ranges currently in existence. This will be the main force behind the growth of the 5G wireless network (Barneto et al. (2020)).

Huo et al. (2019) suggested a framework for mm-wave distributed phased arrays (DPA) and proof-of-concept (PoC) layouts for unmanned aerial vehicles (UAVs) and user equipment (UE) that would be utilized in 5G wireless systems. The UE PoC reaches a maximum downstream rate of more than 4.2 Mbps with optimal heat transport efficiency by allowing a multi stream multi-beam network model (Wu et al. (2018)). Modern commercial and non-commercial wireless communication infrastructure will need multi-beam antennas as basic requirements. Such antennae's many beams can make it possible for different coastal, aerial, and space-based nodes in the network to dynamically link with one another. Quasi-optical methods are anticipated to take over the designing of elevated multi-beam antennas when functioning frequencies exceeding fifth- and sixth-generation technologies rise to the extreme millimeter wave and terahertz ranges (Chukhno et al. (2021)).

Sultan et al. (2022) discussed a dual-band antenna design that has an extremely high frequency-to-size proportion that may be appropriate for combined 4G/mm-wave 5th or even beyond 5G technologies for Internet of Things (IoT) devices. These antennas are built around a narrowed slot that functions as an elevated antenna system at specific energies and a resonated open-ended slotted at low frequencies. Advanced Wireless communication technologies will grow faster with integrated and geographically dispersed Synthesis Phased-Array Antenna and Smart Multi-beam Antenna devices (Ngai and Shavit (2022)). For movable components like robots, autonomous cars, and certain other robotics rescue tools, these are particularly effective. The functioning of these devices in harsh settings where connection to the networks must be

maintained necessitates their enclosing in modern hi-tech radome substances for efficient maintenance and breakage prevention (Fu et al. (2021)).

Ishfaq et al. (2021) demonstrated a broad scanning multi beam PIEA (planar inverted-E antenna) system for vehicular networks. The grid components' enclosed spaces result in significant cross-polarization and mutual coupling at broader scanning orientations. Instead of using switching devices or standard crossings, a limited miniature wideband 4 x 4 circuit is created to supply the microstrip antenna. Najafabadi et al. (2022) offered a concept for a multi beam, inexpensive, antenna array system comprised of butler matrices and two branch-line connectors. The suggested topology uses a new input mechanism that enables the system to provide 7 rays for the butler matrix and 3 rays for the branch-line connector, as opposed to the standard butler array and branch-line combiner, which might typically generate 4 and 2 beams, separately.

Problem statement

When additional beams are sent, the speed of the multi-beam antennas is restricted. This has a significant negative impact on communications. The effectiveness of the communication network might decline as a result of the reduced speed. So, for 5G communication networks, we proposed the Convex Time Modulated Particle Swarm Optimization (CTM-PSO) technique.

3. Proposed Model

In this research, we offer a unique beam-forming optimization technique that reduces transmission beam disturbance while concurrently assuring a specific beam-generated transmission quality to enhance the efficiency of 5G technology. Figure 1 mechanism of suggested strategy.

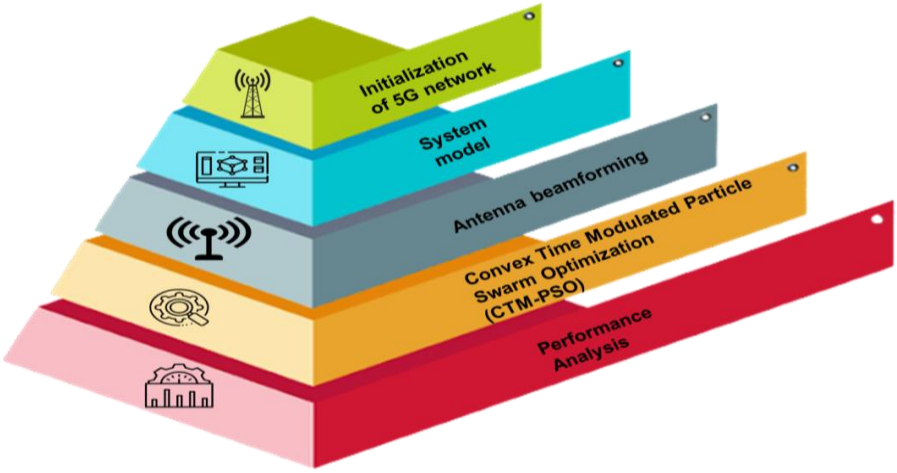

Figure 1: Mechanism of the suggested strategy

Initialization of 5G network

While the development of 5G technology has become underway, to ensure operation, the installation of a 5G broadband network for public users will need the delivery of remote monitoring. Therefore, to transfer data properly, it'll be necessary to establish a fast 5G network. MIMO transmitters, which contain a massive amount of antenna links or components, will be employed by 5G to broadcast and collect additional data concurrently. More consumers may utilize the network at once by increasing overall performance which is advantageous to consumers. Figure 2 illustrates the initialization of the 5G network

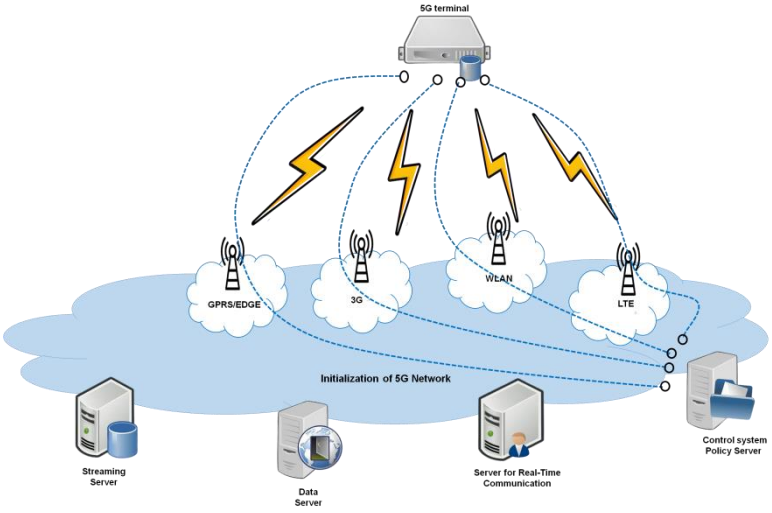

Figure 2: Initialization of 5G network

System model

In this study, identical to, we consider that system operation is carried out in the bottom unit (gNB) of a 5G system by using the well-known downlink transmission configuration s. (t). We work toward a novel capability that would allow the gNB to detect the surroundings concurrently with a directed and adjustable beam whereas another directive wavelength is made aside for the transmission connection. Assuming a singular sharing uniformity linear array (ULA) for TX and RX with N antenna arrays equally separated at half the wavelengths and using a planar waveform, we also take into account distinct RF beam formation weight for TX and RX.

Antenna beamforming

The gNB phased-array readings exhibit well-known arrays responsiveness.

$$a(\theta) = \left[1, e^{j\pi \sin(\theta),\ldots,e^{j\pi (\mathrm{M}-1)\sin(\theta)}}\right]^T \quad (1)$$

where is either the angle of arrival (AoA), denoted by rx, or the angle of departure (AoD), denoted by tx. Equation 2 may therefore be used to represent the spatiotemporal pattern that was emitted at time t.

$$X(t) = s(t)W_{tx} \quad (2)$$

And the TX beam-forming vector is represented by W_{tx} . The spatial signal that was radiated, $X(t)$, then moves through the air and connects with one or more objects, causing refraction that will be gathered for processing by the gNB receiver equipment. Equation 3 may be used to characterize the receiving spatially waveform for K objects.

$$y(t) = \sum_{k=0}^{K-1} b_k e^{2\pi j f_{D,k} t} a(\theta_{rx,k}) a^T(\theta_{rx,k}) X(t - T_k) + n(t) \quad (3)$$

where k and $f_{D,k}{}^t$ represent the kth target's proportional latency and Doppler shift, correspondingly, and bk represents the kth reflection's attenuated coefficient. The noise vector has the prefix $n(t)$. For the sake of convenience, it should be highlighted that complete isolation between the TX and RX devices is maintained in this study, although attainable separation is defined using realistic approaches. Following that, beam forming is used on the receiver end to combine all of the information from every array member, as shown in equation 4.

$$y(t) = W_{rx}^T y(t) \quad (4)$$

Comparison of the TX waveform s(t) with the beamformed RX waveform y allows for the detection of targets (t). The matching filter (MF) operation, which optimizes the signal-to-noise ratio (SNR) of the obtained reflection, is the traditional method for estimating range. It is emphasized that systems relying on frequency computing may also use more specialized and effective methodologies. Generally, dependent on the hardware platforms, some restrictions apply to the TX and RX beamforming values. The RF beamforming parameters are written in equation 5 for convenience.

$$W_{rx} = \left[\alpha_{rx,0} e^{j\beta_{rx,0}}, \ldots, \alpha_{rx,} N - 1 e^{j\beta_{rx,N-1}}\right]^T \quad (5)$$

where the TX and RX magnitude values of the nth antenna structure equate, respectfully, to $tx, n = txn\ and\ tx, n = (rx)n$, and where n is the number of elements in the antenna. Equivalent

expressions for the TX and RX stage alterations at the nth antenna are $tx,n = (tx)n\ and\ rx,n = (rx)n$. The three situations and associated beamforming-related component designs are discussed in this article about beamforming enhancement: The amplitudes tx,n and rx,n are assumed to be substantially equal and continuous for all n in the first consideration of an array design that only permits the phasing management of TX and RX components. This is an example of typical phased-array computation. Finally, we also take into consideration the most adaptable array design providing complete, unrestricted magnitude and phase control of both TX and RX components.

Convex Time Modulated Particle Swarm Optimization (CTM-PSO)

The initial non-convex difficulty can be effectively handled by a two-step convex solution that has been presented thanks to the reduction in the size of the acceptable area for the time modulation design. During the first phase, the form of the sequence at the central wavelength is determined by optimizing w0 by the SLL constraint that has been given. In this context, w0 refers to the equivalent stimulation at the central wavelength that was covered in the second stage. The first step may be represented mathematically using equation 6.

$$\begin{cases} \min\limits_{w^0 \epsilon C^{N,1}} -real(a(\theta_0)^T V^0) \\ s.t.\ \ image(a(\theta_0)^T V^0) = 0 \\ |aa(\theta_i)^T w^0| \le SLL \cdot real(a(\theta_0)^T V^0), \theta_i \epsilon \Theta_{SL} \\ |V^0| \le [1]_{N\times 1} \\ real(V^0) \ge [I_l \cdot b]_{N\times 1} \end{cases} \tag{6}$$

where 0 is the direction of the primary beam, SL denotes the sidelobe area that is being considered, SLL denotes the SLL restriction that has been specified, and $real(\cdot)$ and $imag(\cdot)$ denote the real and imaginary operations, accordingly. In the final inequality requirement, real (V^0) is employed to make an approximation of $|V^0|$ to guarantee that the difficulty with the response is convex. In stage two, which is conducted based on the w0 that was acquired in phase one, the goal is to reduce the SBL by maximizing V^1, which can be represented as 7.

$$\begin{cases} \min\limits_{SBL \epsilon R^+, w^1 \epsilon C^{N,1}} SBL \\ s.t. \quad |a(\theta_i)^T V^1| \le SBL, \theta_i \in \Theta_{all} \\ |aa(\theta_i)^T V^0| \le SLL \cdot real(a(\theta_0)^T w^0), \theta_i \epsilon \Theta_{SL} \\ |V^1| \le |V^0| \circ sinc(\pi \tau_{min}) \\ real(V^1) \ge |V^0| \circ sinc(\pi \tau_{max}) \end{cases} \tag{7}$$

where SBL is a loose constant, (all) denotes the circular area in all dimensions, and (°) is the Hadamard derivative. $\tau min = [\tau n, min]\, N \times 1$ and $\tau max = [\tau n, max]\, N1$ are two horizontal matrices that are used to limit the range of, and their values may be determined using the equation $[n, min, n, max] = [|V^0 n|, |V^0 n|/Il]\, [b, 1]$. The convexity of the equation is maintained by approximating the value of $|V^1|$ with real (V^1) in this last inversion constraint, which does, however, result in a smaller area that is viable to solve. After w0 and w1 have been found, the TMA activation I, t may be calculated using the following formula, with pha () serving as the process generator denoted in equation 8.

$$\frac{|W_n^1|}{|W_n^0|} = \left|\frac{sin(\pi\tau_n)}{\pi\tau_n}\right|,\ I_n = \frac{W_n^1}{\tau_n}, t_n = \frac{pha(W_n^0) - phaW_n^1 - \pi\tau_n}{2\pi} \quad (8)$$

When a certain SLL condition is provided, the low SBL time modulation beam creation may be easily addressed by using the convex solver that is readily accessible. It is possible to accomplish the optimizing procedure in only a few minutes for a 100-element constant time modulation beam forming, making it incredibly time effective. However, as a result of the presented simplifications, the workable area has been lowered. As a result of this, it is not possible to ensure that the solution will be desirable for the convex strategy. Furthermore, this method is limited to single-objective enhancement with an existing medicated SLL and side lobe region. When there are a considerable number of CTM beam formation elements, such as 50 elements (75 factors), the search area for optimization is much very difficult to navigate. When using a population-relying optimization technique, it is common knowledge that a complex selection area with a huge number of varying factors requires typically requires more population to assure the optimal approach. This also means that the algorithmic responsibility will be significantly enhanced. When there are a considerable number of CTM beam creation elements, such as 50 elements (75 factors), the search area for optimization is much very difficult to navigate. When using a population-relying optimization technique, it is common knowledge that a complex selection area with a huge number of varying factors requires typically requires more population to assure the optimal approach. This also means that the algorithmic responsibility will be significantly enhanced. Moreover, with a little background expertise in the selection area and by declaring the finest utilization of the convexity of the remedy issue, a few useful citation marks with broad scatter PSO can be introduced in the community to discover the inquiry around the most responsible portion of the selection area, that is extremely helpful for enhancing both the reliability of the remedy and the effectiveness of the method. When compared with other methods that are currently available, this approach is one of the more effective ways to solve

relatively large-scale CTM beam creation issues while working within a constrained computing constraint. An effective combination approach is developed using the sequence depicted in Figure 3 in an attempt to cope with the relatively broad range CTM beam creation issue while adhering to a constrained computing constraint. PSO is used in the suggested technique to develop a set of standard elements for the Pareto front.

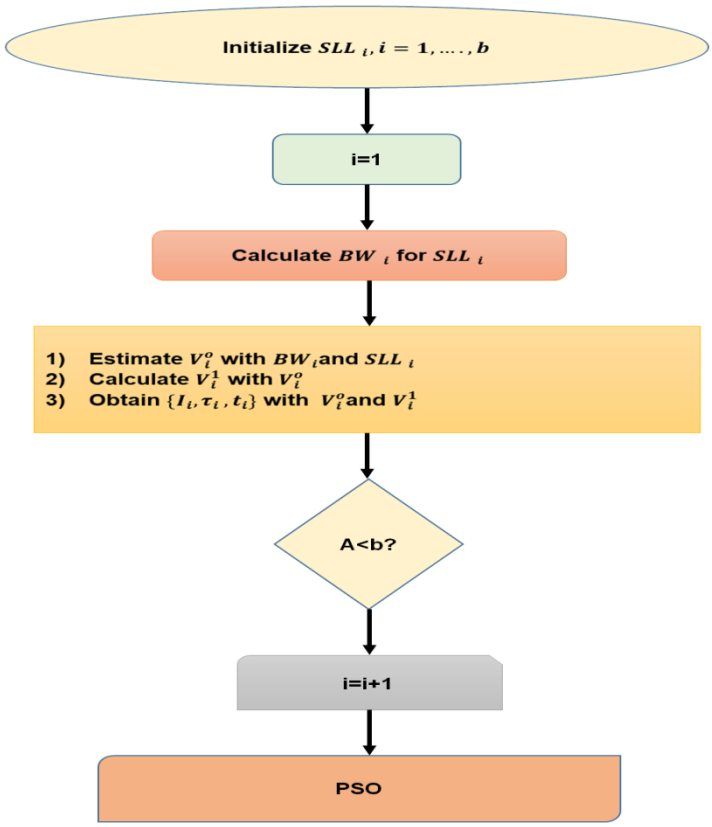

Figure 3: Flowchart of the proposed technique

These benchmark elements are then inserted into the populace of PSO to enhance the efficiency of the response and speed resolution of the CTM beam construction. Due to the underlying factors and factors, the CTM technique is employed to create the points of reference:

1) A quick pace of response because only two CP issues need to be solved for each reference point, which is advantageous for the generation of a collection of points. In addition, the quality of the solutions offered by the points still offers considerable scope for the investigation of PSO.
2) The SLL is founded on a predetermined value, which may be used to construct a group of points spanning a vast SLL range. These points can then be used to determine the SLL. This is particularly helpful for advancing the Pareto front since it improves the dispersion of the front. In

the CTM beam formation section, when a referral SLLi is provided, a side lobe area called SL has to be pre-decided to complete the first step of the CTM beam formation process. In most cases, the decision on the area known as SL on the side lobe is made manually. A method for automatically determining the reference side lobe area for CTM is presented here as one of our hypotheses. Equation 9 may be used to calculate the initial null beam width BWi (rad) for a Chebyshev taper for a linear combination consisting of 2N elements that have a certain SLLi (in dB). Algorithm 1 shows the procedure of PSO.

$$BW_i = 2sin^{-1}\left\{\frac{1}{\pi\beta d}cos^{-1}\left[\frac{1}{x_0}cos\left(\frac{\pi/2}{2N-1}\right)\right]\right\} \quad (9)$$

$$where\ x_0 = cosh\left(\frac{cos^{-1}\left(10^{-SLL_i/20}\right)}{2N-1}\right)$$

Algorithm 1: PSO

Create the PSO's first population from the beginning.

Place the reference locations for the Pareto front within the population.

$G = 1$, component speeds, personal best positions, the absence of a dominant repository, and hypercubes of the search space should all be initialized.

Make adjustments to the velocity of each particle.

Determine the new location of each particle by computing it.

Conduct an analysis of the SLL and SBL performance for each particle.

Perform an update on the position of each particle, as well as their personal bests, the repository, and the hypercubes.

$G < G_{max}?, G = G + 1$

Maintain the solutions in the repository so that an optimized Pareto front may be created.

4. Performance Analysis

In this article, we suggested an optimization algorithm for 5G communication networks, offering multiple concurrent transceivers to support efficient beamformed interactions. In this section, we analyze the results for the metrics such as scanning performance, scanning loss, gain, radiation pattern, and amplitude versus frequency. The existing approaches are deep beam, artificial bee colony algorithm, maximum power transmission efficiency, and generalized joined coupler.

A. Scanning performance

An estimation of the real spacecraft location is made by adding scanning motions to a monitoring antenna's track. The periodic transverse motions of an antenna make up the detector activities. The transmitted signal's strength changes as a result of such movement and are utilized to infer the spacecraft's location. Figure 4 presented the scanning performance of the proposed antenna. The existing approach such as DB has attained 50%, ABCA has achieved 70%, MPTE has accompanied 65%, and GJC has attained 82%. The proposed approach attained 96%. Table 1 depicts the measuring values of scanning performance.

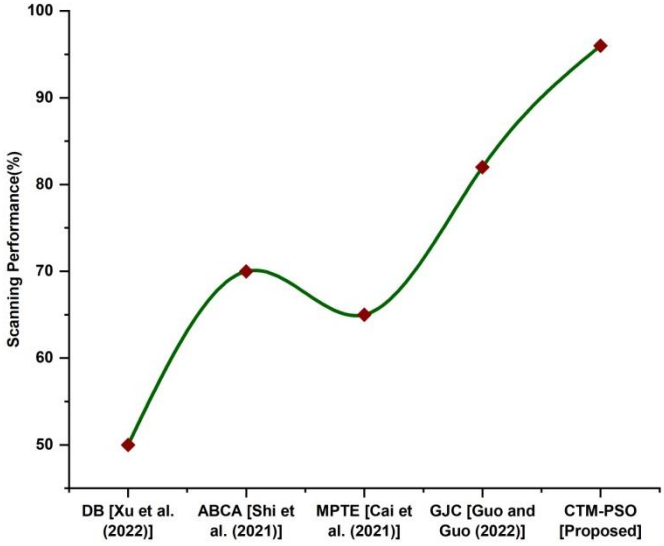

Figure 4: Analysis of scanning performance

Table 1: Comparative values of scanning performance

Techniques	Scanning Performance (%)
DB	50
ABCA	70
MPTE	65
GJC	82
CTM-PSO [Proposed]	96

B. Scanning loss

Whenever a navigation system uses scanning antennas, the penetration is lower than when the beam is always pointed at the destination since the antenna scans over the destination. Figure 5 displays the antenna's optimum scanning losses together with the intended values for the transmitter and receiver bands in the frequency range. The proposed approach has a scanning

loss of 50% whereas the existing techniques such as DB have attained 72%, ABCA has achieved 42%, MPTE has accompanied 67%, and GJC has attained 98%.

$$SC = 10^{*}\log\left(cos^{n}(\theta)\right) power \quad (10)$$

When n is a constant and θ is the scanning angle of the corresponding point direction of the antenna. Table 2 shows the measuring values of scanning loss.

Table 2: Comparative values of scanning loss

Techniques	Antenna Scanning Loss (%)
DB	85
ABCA	62
MPTE	54
GJC	79
CTM-PSO [Proposed]	42

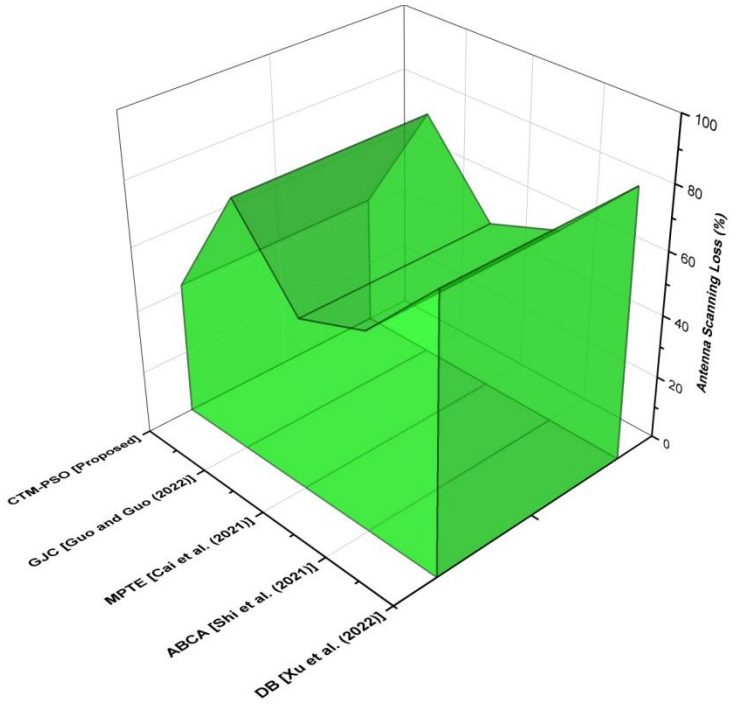

Figure 5: Antenna scanning loss analysis

C. Gain

The capability of an antenna to emit less or more energy in any direction as contrasted to hypothetical antennas is known as antenna gain. An antenna could transmit evenly throughout all directions when it was constructed as a suitable spherical. Greater energy transmission to the receivers via greater antennae strengthens the data it received. Large antennas may also make broadcast signals a hundred times faster by absorbing additional radiation when employed as receivers due to their complementarity. In Figure 6, the antenna gain is shown. The suggested methodology achieved a 99% gain in contrast to current approaches such as DB, ABCA, MPTE, and GJC which have achieved 52%, 42%, 62%, and 82% gains. Table 3 indicates the measuring values of gain.

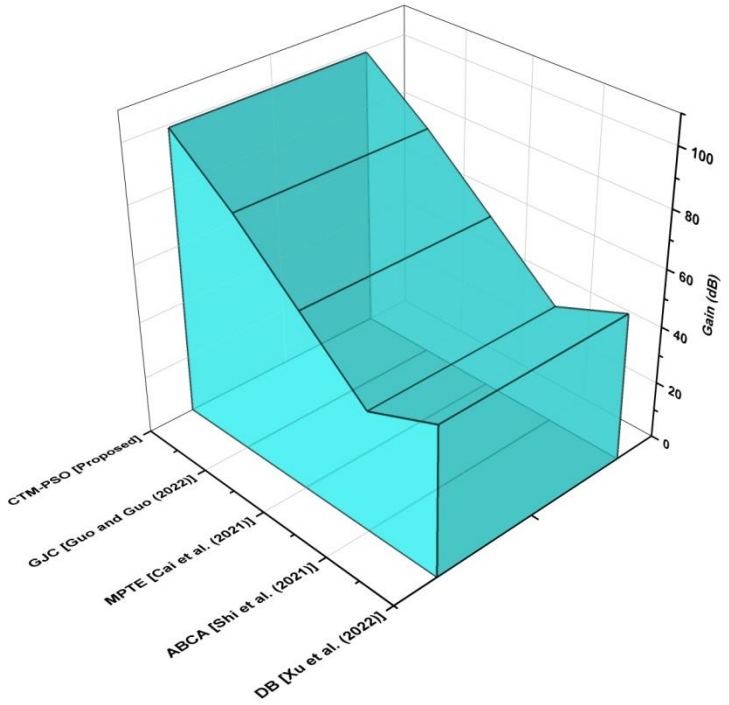

Figure 6: Analysis of antenna gain

Table 3: Comparative values of gain

Techniques	Gain (dB)
DB	52
ABCA	42
MPTE	62
GJC	82
CTM-PSO [Proposed]	99

D. Radiation pattern

The word radiation pattern refers to a visual representation of the broad variety with the greatest dimension of the directional antenna's radiation characteristics as a result of the magnetic wave's propagation path. The power emitted per unit solid angle is determined by the radiation intensity, which is crucial for the antenna system. In Figure 7, the radiation pattern is shown. Table 4 illustrates the measures of the radiation pattern.

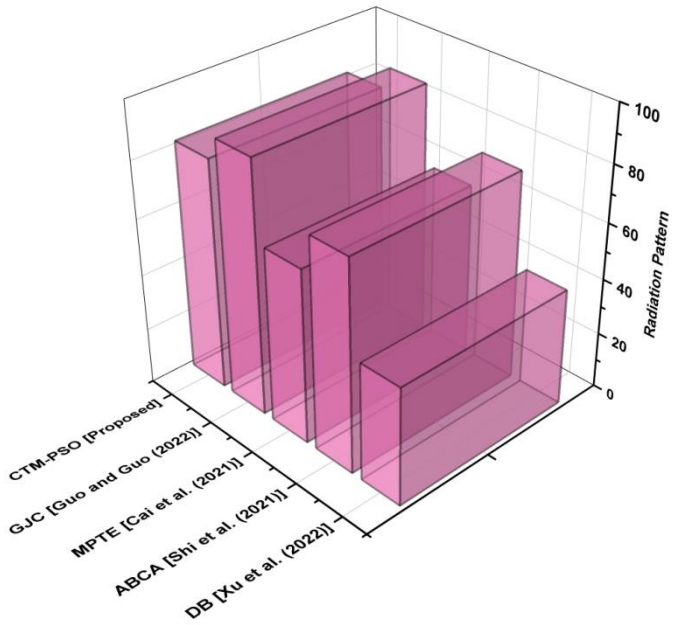

Figure 7: Radiation pattern

Table 4: Measures of the radiation pattern

Techniques	Radiation Pattern
DB	42
ABCA	75
MPTE	62
GJC	90
CTM-PSO [Proposed]	82

E. Amplitude vs. frequency

The amplitude of an antenna is the area it travels between its equilibrium position and its highest departure. The quantity of a beam's iterations in a second is referred to as its frequency. It has a transmitting capacity and functions as a frequency filter. Enhanced precision is produced at specific frequencies; however, the penetration depth is restricted. Figure 8 shows the amplitude of frequency. Table 5 demonstrates the values of amplitude and frequency.

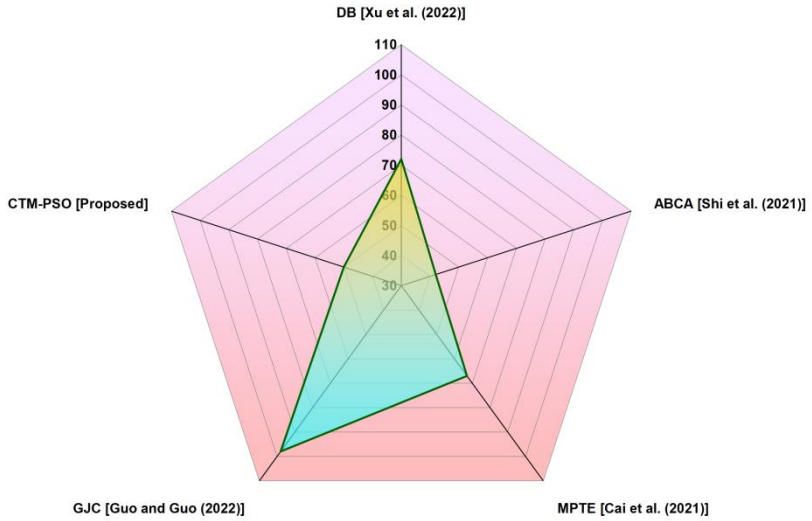

Figure 8: Amplitude vs. frequency

Table 5: Measures of amplitude and frequency

Techniques	Amplitude Frequency
DB	72
ABCA	42
MPTE	67
GJC	98
CTM-PSO [Proposed]	50

5. Conclusion

A multi-beam antenna, often known as an MBA, is an antenna that can create numerous independent beams concurrently from such a unique field. Utilizing high-gain spot beams that overlapped one another, often offers constant review throughout a predetermined range of vision. Maximizing the minimal yield while remaining inside the service area is the overarching goal of the system design overall MBAs. In this paper, we proposed a novel beamforming design and optimization approach based on the Convex Time Modulated Particle Swarm Optimization (CTM-PSO) to give the immense potential for representing the high operational and maintenance for promoting beamforming and enormous MIMO for 5G communication systems. The findings are analyzed, and we end up with important outcomes. As a direct consequence of this, the efficacy of this antenna system is approximately 96%, which enables it to provide useful outcomes.

Acknowledgment: The authors appreciate the Deanship of Scientific Research at the King SaudUniversity represented by the Research Center at CBA for financially supporting this research.

References

1. Dangi, R., Lalwani, P., Choudhary, G., You, I. and Pau, G., 2021. Study and investigation on 5G technology: A systematic review. Sensors, 22(1), p.26.
2. Miladić-Tešić, S., Marković, G., Peraković, D. and Cvitić, I., 2022. A review of optical networking technologies supporting 5G communication infrastructure. Wireless Networks, 28(1), pp.459-467.
3. Njoku, J.N., Nwakanma, C.I. and Kim, D.S., 2022, October. The Role of 5G Wireless Communication System in the Metaverse. In 2022 27th Asia Pacific Conference on Communications (APCC) (pp. 290-294). IEEE.
4. Guo, Y.J., Ansari, M., Ziolkowski, R.W. and Fonseca, N.J., 2021. Quasi-optical multi-beam antenna technologies for B5G and 6G mmWave and THz networks: A review. IEEE Open Journal of Antennas and Propagation
5. Guo, Y.J., Ansari, M. and Fonseca, N.J., 2021. Circuit-type multiple beamforming networks for antenna arrays in 5G and 6G terrestrial and non-terrestrial networks. IEEE Journal of Microwaves, 1(3), pp.704-722.
6. Guo, Y.J. and Ziolkowski, R.W. eds., 2022. Antenna and Array Technologies for Future Wireless Ecosystems. John Wiley & Sons.
7. Aslan, Y., Roederer, A., Fonseca, N.J., Angeletti, P. and Yarovoy, A., 2021. Orthogonal versus zero-forced beamforming in multibeam antenna systems: review and challenges for future wireless networks. IEEE Journal of Microwaves.
8. Ruggerini, G., Nicolaci, P.G., Toso, G. and Angeletti, P., 2019. A Ka-Band Active Aperiodic Constrained Lens Antenna for Multibeam Applications: Active discrete lens antennas are promising alternative solutions for multibeam coverage using a single aperture. IEEE Antennas and Propagation Magazine, 61(5), pp.60-68.
9. Vallappil, A.K., Rahim, M.K.A., Khawaja, B.A., Murad, N.A. and Mustapha, M.G., 2020. Butler matrix based beamforming networks for phased array antenna systems: A comprehensive review and future directions for 5G applications. IEEE Access, 9, pp.3970-3987.

10. Barneto, C.B., Liyanaarachchi, S.D., Riihonen, T., Anttila, L. and Valkama, M., 2020, June. Multibeam design for joint communication and sensing in 5G new radio networks. In ICC 2020-2020 IEEE International Conference on Communications (ICC) (pp. 1-6). IEEE.
11. Huo, Y., Lu, F., Wu, F. and Dong, X., 2019, September. Multi-beam multi-stream communications for 5G and beyond mobile user equipment and UAV proof of concept designs. In 2019 IEEE 90th Vehicular Technology Conference (VTC2019-Fall) (pp. 1-5). IEEE.
12. Wu, Q., Hirokawa, J., Yin, J., Yu, C., Wang, H. and Hong, W., 2018. Millimeter-wave multibeam endfire dual-circularly polarized antenna array for 5G wireless applications. IEEE transactions on antennas and propagation, 66(9), pp.4930-4935.
13. Chukhno, N., Chukhno, O., Moltchanov, D., Molinaro, A., Gaidamaka, Y., Samouylov, K., Koucheryavy, Y. and Araniti, G., 2021. Optimal Multicasting in Millimeter Wave 5G NR with Multi-beam Directional Antennas. IEEE Transactions on Mobile Computing.
14. Sultan, K., Ikram, M. and Nguyen-Trong, N., 2022. A Multiband Multibeam Antenna for Sub-6 GHz and mm-Wave 5G Applications. IEEE Antennas and Wireless Propagation Letters, 21(6), pp.1278-1282.
15. Ngai, E.C., and Shavit, R., 2022, July. Leading Edge Synthetic Phased-Array (SPA) Antenna and Smart Multi-beam Antenna Sensors for Massive MIMO Mobile-Wireless Networks. In 2022 IEEE International Symposium on Antennas and Propagation and USNC-URSI Radio Science Meeting (AP-S/URSI) (pp. 1862-1863). IEEE.
16. Fu, P., Zhang, Y. and Li, Y., 2021, November. A Novel Integrated Multi-Beam Antenna Array for Low-complex Massive MIMO Base Station. In 2021 IEEE International Workshop on Electromagnetics: Applications and Student Innovation Competition (iWEM) (pp. 1-3). IEEE.
17. Ishfaq, M.K., Babale, S.A., Chattha, H.T., Himdi, M., Raza, A., Younas, M., Rahman, T.A., Rahim, S.K.A. and Khawaja, B.A., 2021. Compact Wide-Angle Scanning Multibeam Antenna Array for V2X Communications. IEEE Antennas and Wireless Propagation Letters, 20(11), pp.2141-2145.
18. Najafabadi, A.M.A., Ghani, F.A. and Tekin, I., 2022. Low-cost multibeam millimeter-wave array antennas for 5 G mobile applications. IEEE Transactions on Vehicular Technology.
19. Xu, G., Tan, F., Ran, Y., Zhao, Y. and Luo, J., 2022. Joint Beam-Hopping Scheduling and Coverage Control in Multibeam Satellite Systems. IEEE Wireless Communications Letters.

20. Shi, Z., Zhang, X., Yu, F. and Gao, M., 2021, July. Optimal Design of Shaped Multiple-Beam Antenna Based on Artificial Bee Colony Algorithm. In Journal of Physics: Conference Series (Vol. 1971, No. 1, p. 012028). IOP Publishing.
21. Cai, X., Gao, T., Dong, Y. and Wen, G., 2021, May. Optimal Design of Multi-beam Antenna Array by the Method of Maximum Power Transmission Efficiency. In 2021 International Conference on Microwave and Millimeter Wave Technology (ICMMT) (pp. 1-3). IEEE.
22. Guo, C.A. and Guo, Y.J., 2022. A General Approach for Synthesizing Multibeam Antenna Arrays Employing Generalized Joined Coupler Matrix. IEEE Transactions on Antennas and Propagation, 70(9), pp.7556-7564.